

## Hierarchical magnetic core-shell nanostructures for microwave absorption: Synthesis, microstructure and property studies

LIU JiWei<sup>1,2</sup>, XU JunJie<sup>1</sup>, LIU ZhengWang<sup>1</sup>, LIU XiaLin<sup>1</sup> & CHE RenChao<sup>1\*</sup>

<sup>1</sup>Department of Materials Science and Laboratory of Advanced Materials, Fudan University, Shanghai 200438, China;

<sup>2</sup>National Institute for Materials Science (NIMS), Sengen 1-2-1, Tsukuba, Ibaraki 305-0047, Japan

Received August 5, 2013; accepted September 24, 2013; published online November 4, 2013

Core-shell nanostructures have attracted considerable attention in the past decades because of their fundamental scientific significance and many technological applications. Recently, it has been reported that the core-shell nanostructures with advanced compositions and complicated morphologies show great potential as high-performance microwave absorbers due to their unique properties, such as large surface areas, multi-functionalities and synergistic effects between the interior core and outer shell. This review article focuses on the recent progress in synthesis and characterization of hierarchical magnetic core-shell nanostructures for microwave absorption applications based on our own work. In addition, several future trends in this field for next-generation microwave absorbers are discussed.

**magnetite, core-shell, hierarchical, hydrothermal synthesis, microstructure, microwave absorption**

### 1 Introduction

Over the past decades, the synthesis and characterization of advanced nanostructured materials have become a particularly important area of research and have received a growing interest in chemistry, materials science, and biology [1, 2]. Among numerous novel nanostructured materials, core-shell nanostructures (CSNs) have been subjected to extensive study for the combined functionalities of core and shell and enhanced properties or synergistic effects between the components (Figure 1(a)). Moreover, the CSNs can be widely used as templates for the synthesis of yolk-shell nanostructures (YSNs), which represent a special class of CSNs with distinctive core@void@shell configuration (Figure 1(b)). Due to their unique properties such as low density, large surface area, functional interior core, designable interstitial void, useful outer shell, the YSNs have recently attracted considerable attention in a wide range of applica-

tions including catalysis, energy storage and conversion, drug delivery, and so on [3–6]. Notwithstanding the advances made in fabrication techniques and materials science, one of the great challenges in this field is how to design and prepare the structure with various functions such as catalytic, electronic, and magnetic properties as well as low toxicity and high stability for desired applications [7, 8].

Microwave absorbers are of great importance to solve the expanding electromagnetic interference (EMI) problems caused by the development of wireless communications, digital systems, and fast processors. As an ideal microwave absorber, one must satisfy two prerequisites: (1) the impedance matching between the material surface and free space, which requires the complex permittivity close to complex permeability; (2) the incident microwaves can be absorbed or attenuated by the material as much as possible, which requires the material with strong magnetic and dielectric loss.

In spite of extensive research efforts, it is still an urgent task to develop facile and feasible routes for synthesizing novel high-efficient microwave absorbers with lightweight,

\*Corresponding author (email: rcche@fudan.edu.cn)

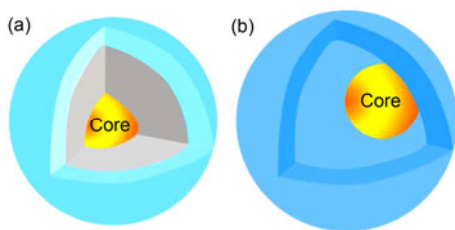


**Figure 1** Schematic illustration of CSN (a) and YSN (b).

thin thickness, wide absorption bandwidth, and strong absorption characteristics for innovative EMI shielding in military, industrial, and commercial field [9–11]. Intensive studies in the past have proven that the absorption performance of the microwave absorbers is strongly affected by the permittivity ( $\epsilon$ ) and permeability ( $\mu$ ) that depend on the size, composition, microstructure, and morphology [12]. Recent advances show that excellent microwave absorption properties can be obtained from hierarchical nanostructures with complicated geometrical morphologies [13]. It has also been demonstrated that core-shell structured nanocomposites show great potential for broadband lightweight microwave absorbers with lower reflection loss than the pure core or shell materials [14–16]. It is noteworthy that in many cases the outer shells not only stabilize the inner cores, but can also cause enhanced properties or satisfactory synergistic effects, providing tremendous opportunities for achieving excellent microwave absorption performance.

In this review article, we report our recent work on the synthesis, microstructure, and microwave absorption properties of hierarchical  $\text{Fe}_3\text{O}_4$ -based CSNs and YSNs, followed by a brief discussion on the current issues and new trend in this field.

## 2 Core-shell microspheres with $\text{Fe}_3\text{O}_4$ cores and nanosheet-assembled $\text{TiO}_2$ shells

As an important class of functional nanomaterials,  $\text{Fe}_3\text{O}_4$  has long been studied as microwave absorbers because of its ease of synthesis, low cost, and strong absorption characteristics [17]. However, the  $\text{Fe}_3\text{O}_4$  materials usually suffer from rapid oxidation, high density, and narrow absorption bandwidth, which restrict their further applications.  $\text{TiO}_2$  is one of the most extensively investigated functional metal oxides because of its fascinating features, such as good chemical and thermal stability, excellent electronic and optical properties [18]. The incorporation of the dielectric  $\text{TiO}_2$  into the  $\text{Fe}_3\text{O}_4$ -based microwave absorber may generate a high dielectric constant and loss due to effective interfaces between the dielectric and magnetic materials, which have an advantage in the area of matching complex permittivity and permeability by adjusting the component and morphology [19]. Therefore, it will be of significance to

synthesize core-shell structures with unique morphologies and combined dielectric-magnetic characteristics and to study the relationship between the core-shell structures and their absorption performance for the development of highly efficient microwave absorbers.

Recently, we reported a solvothermal reaction for the synthesis of multifunctional core-shell microspheres with  $\text{Fe}_3\text{O}_4$  cores and nanosheet-assembled  $\text{TiO}_2$  shells [20]. Field-emission scanning electron microscopy (FESEM) shown in Figure 2(a) indicated that the flower-like microsphere was composed of numerous ultrathin nanosheets. Transmission electron microscopy (TEM) image shows that the microspheres possess a core-shell structure with nanosheet-assembled shells (Figure 2(b)). The as-synthesized core-shell microspheres were further examined by electron energy loss spectroscopy (EELS). It could be clearly seen in Figure 2(c) that these core-shell microspheres were composed of a  $\text{Fe}_3\text{O}_4$  core and  $\text{TiO}_2$  nanosheet shells. Interestingly, the  $\text{Fe}_3\text{O}_4@ \text{TiO}_2$  core-shell microspheres with different  $\text{Fe}_3\text{O}_4$  core size and  $\text{TiO}_2$  shell thickness can be easily synthesized by simply varying the synthetic parameters.

In order to estimate the enhanced absorption performance for the  $\text{Fe}_3\text{O}_4@ \text{TiO}_2$  core-shell microspheres, the complex permittivity and permeability of both the  $\text{Fe}_3\text{O}_4$  and  $\text{Fe}_3\text{O}_4@ \text{TiO}_2$  core-shell microspheres were investigated (Figure 2(d, e)). The electromagnetic data indicate that the complex permittivity and permeability of these nanostructures can be optimized to improve their absorption performance. As shown in Figure 2(f), the  $\text{Fe}_3\text{O}_4@ \text{TiO}_2$  core-shell microspheres exhibited lower reflection loss and wider absorption bandwidth than pure  $\text{Fe}_3\text{O}_4$ . Note that the maximum reflection loss value of the  $\text{Fe}_3\text{O}_4@ \text{TiO}_2$  core-shell microspheres with 400-nm  $\text{Fe}_3\text{O}_4$  cores and 150-nm  $\text{TiO}_2$  shells is  $-23.3$  dB at 7 GHz with a thickness of 2 mm. The enhanced microwave absorption properties of the  $\text{Fe}_3\text{O}_4@ \text{TiO}_2$  microspheres might stem from the core-shell structure and ultrathin nanosheet-assembled  $\text{TiO}_2$  shells that increased the geometrical absorption/scattering effect, while the relatively large specific surface area ( $48 \text{ m}^2 \text{ g}^{-1}$ ) and high porosity ( $0.15 \text{ cm}^3 \text{ g}^{-1}$ ) could provide more active sites for the reflection and scattering of electromagnetic waves. Importantly, effective complementarities between the dielectric loss and magnetic loss can be realized by tuning the  $\text{Fe}_3\text{O}_4$  core size and  $\text{TiO}_2$  shell thickness, thus resulting in the significantly enhanced microwave absorption properties.

## 3 Yolk-shell microspheres with $\text{Fe}_3\text{O}_4$ cores and nanosheet-assembled $\text{TiO}_2$ shells

As an important extension of CSNs, yolk-shell structured materials have attracted more and more attention due to their fundamental and technological importance. Moreover, YSNs can possess higher surface area, larger void space and

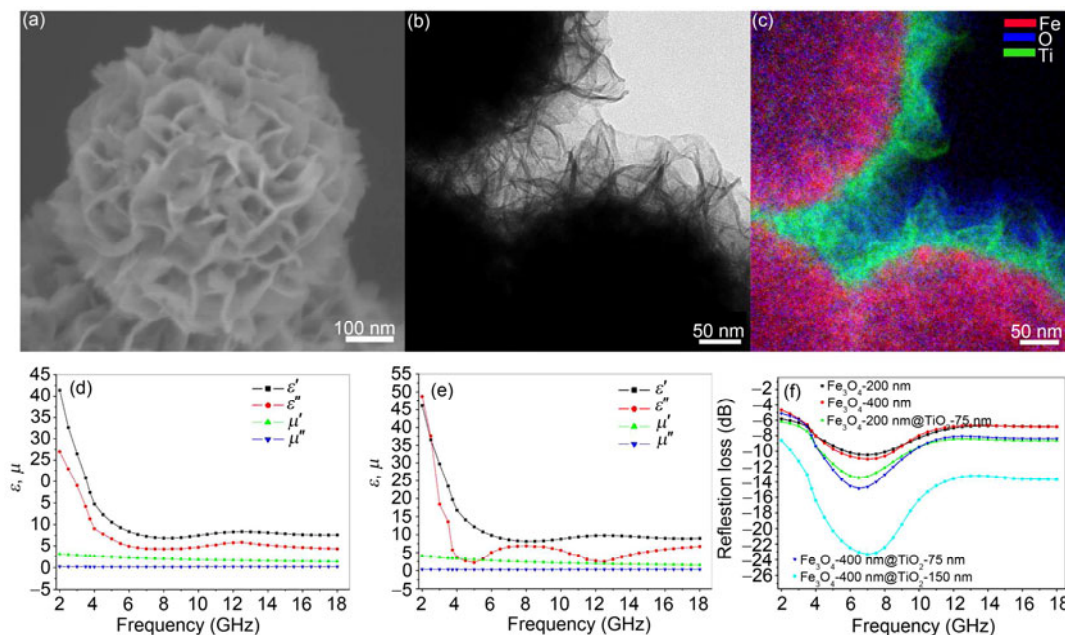


**Figure 2** FESEM (a), TEM (b) and EELS (c) images of the Fe<sub>3</sub>O<sub>4</sub>@TiO<sub>2</sub> core-shell microspheres. Frequency dependence of real (') and imaginary (") parts of complex permittivity and permeability of Fe<sub>3</sub>O<sub>4</sub> (d) and Fe<sub>3</sub>O<sub>4</sub>@TiO<sub>2</sub> core-shell microspheres (e). Microwave reflection loss curves of the Fe<sub>3</sub>O<sub>4</sub> and Fe<sub>3</sub>O<sub>4</sub>@TiO<sub>2</sub> core-shell microspheres (f). (Copyright (2012) John Wiley & Sons)

lower density compared with traditional CSNs. With the integration of the chemical composition and unique structure, the versatile YSNs with low densities and large surface areas are expected to be ideal candidates as absorbers for microwave absorption applications.

On the basis of previously reported Fe<sub>3</sub>O<sub>4</sub>@TiO<sub>2</sub> core-shell microspheres, our group recently reported a facile and efficient strategy for the synthesis of Fe<sub>3</sub>O<sub>4</sub>@TiO<sub>2</sub> yolk-shell microspheres with nanosheet-assembled shells [21]. The experimental procedures could be briefly described as follows: uniform Fe<sub>3</sub>O<sub>4</sub> core particles were first coated with SiO<sub>2</sub> shells and subsequently used as templates to construct Fe<sub>3</sub>O<sub>4</sub>@SiO<sub>2</sub>@TiO<sub>2</sub> microspheres with shells assembled from TiO<sub>2</sub> nanosheets, and finally the inner SiO<sub>2</sub> shells were selectively removed using KOH solution. TEM imaging clearly shows that the synthesized microspheres possess a unique yolk-shell structure, which is composed of a dark core of ~225 nm in diameter encapsulated in a nanosheet-assembled shell of ~885 nm in diameter and ~240 nm in thickness (Figure 3(a)). As shown in Figure 3(b), the yolk-shell structure with a large interstitial void between the core and the shell could be clearly discerned. The shells assembled from nanosheets were lamellar structures about several nm in thickness and a few hundred nm in lateral size diameter. According to the microstructure analysis of the yolk-shell structure, high-magnification TEM, bright-field scanning transmission electron microscopy (BF-STEM), and high angle annular dark-field STEM (HAADF-STEM) images of an individual microsphere combined with line scanning profiles further confirmed that the yolk-shell structure was composed of a Fe<sub>3</sub>O<sub>4</sub> core individually en-

capsulated in ultrathin nanosheet-assembled TiO<sub>2</sub> shells (Figure 3(c–f)). When evaluated as microwave absorbers, the as-synthesized Fe<sub>3</sub>O<sub>4</sub>@TiO<sub>2</sub> yolk-shell microspheres with defined core sizes, interstitial void volumes, and shell thicknesses show clear differences in their microwave absorption properties. The maximum reflection loss value of the Fe<sub>3</sub>O<sub>4</sub>@TiO<sub>2</sub> yolk-shell microspheres can reach –33.4 dB at 7 GHz at a thickness of 2 mm. Moreover, the absorption bandwidths with reflection loss values lower than –10 dB are up to 7.8 GHz. It is believed that the significantly enhanced microwave absorption properties may be attributed to the unique yolk-shell structure with magnetic Fe<sub>3</sub>O<sub>4</sub> cores and hierarchical TiO<sub>2</sub> shells.

#### 4 Yolk-shell microspheres with Fe<sub>3</sub>O<sub>4</sub> cores and nanoneedle-assembled copper silicate shells

To date, numerous approaches based on layer-by-layer assembly [22], electrochemical deposition [23], Kirkendall or Ostwald ripening effect [24], and templating process [25] have been developed to prepare the YSNs. In principle, template-assisted methods have been proven to be general and effective methods for synthesizing a wide range of yolk-shell materials [26]. The provided template is suitably chosen, yolk-shell particles with very different functionalities in their interior cores and outer shells can be engineered. More recently, a variety of products have been prepared by the template-assisted methods and the rational design and construction of yolk-shell particles of well-defined size, composition, structure, and function have been technologi-

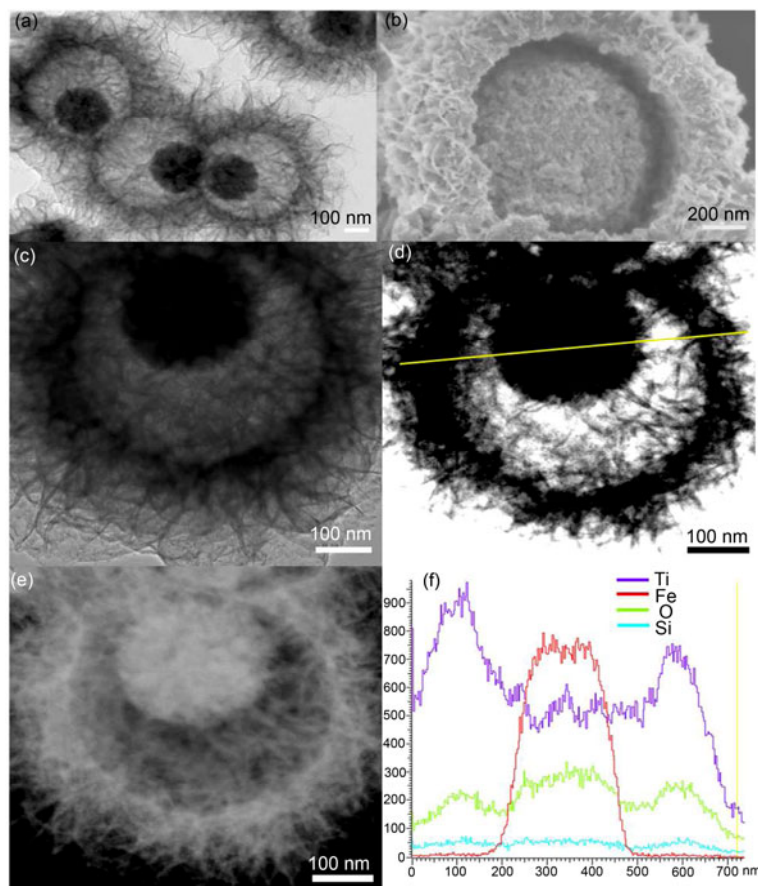


**Figure 3** TEM (a) and FESEM (b) images of the  $\text{Fe}_3\text{O}_4@ \text{TiO}_2$  yolk-shell microspheres. TEM (c), BF-STEM (d), and HAADF-STEM (e) images of an individual yolk-shell microsphere. (f) Line scanning profiles of Fe, O, Ti, and Si recorded along the line shown in (d). (Copyright (2013) American Chemical Society)

cally achieved. However, there have been very few studies on the synthesis and applications of hierarchical yolk-shell structures as microwave absorbers. On the other hand, an understanding of the relationship between the yolk-shell structure and the microwave absorption properties of these materials is therefore necessary in order to optimize the absorption performance.

Following this concept, we demonstrated the synthesis of hierarchical yolk-shell microspheres with magnetic  $\text{Fe}_3\text{O}_4$  cores and nanoneedle-assembled copper silicate shells ( $\text{Fe}_3\text{O}_4@ \text{CuSilicate}$ ) by combining the sol-gel process and hydrothermal reaction [27]. The synthesis approach is schematically illustrated in Figure 4(a). By the classical Stöber method, uniform  $\text{Fe}_3\text{O}_4$  particles were coated with a smooth silica layer to obtain  $\text{Fe}_3\text{O}_4@ \text{SiO}_2$  core-shell microspheres (Figure 4(b–e)). The further hydrothermal treatment of the  $\text{Fe}_3\text{O}_4@ \text{SiO}_2$  core-shell microspheres in  $\text{Cu}^{2+}$  and ammonia solution led to the formation of  $\text{Fe}_3\text{O}_4@ \text{CuSilicate}$  yolk-shell microspheres (Figure 4(f, g)). TEM, BF-STEM and HAADF-STEM images of a representative microsphere combined with line scanning profiles clearly reveal that the yolk-shell structure was composed of a  $\text{Fe}_3\text{O}_4$  core individ-

ually encapsulated in ultrafine nanoneedle-assembled copper silicate shells (Figure 4(h–k)). As parameters that can strongly influence the microwave absorption properties, the size and shell thickness of the  $\text{Fe}_3\text{O}_4@ \text{CuSilicate}$  microspheres could be well controlled by varying the  $\text{Fe}_3\text{O}_4$  core size,  $\text{SiO}_2$  coating thickness, and  $\text{Cu}^{2+}$  concentration. The complex permittivity and permeability of the  $\text{Fe}_3\text{O}_4$  and  $\text{Fe}_3\text{O}_4@ \text{CuSilicate}$  yolk-shell microspheres were investigated to estimate the microwave absorption properties of as-synthesized products. As shown in Figure 5, the relatively high values of imaginary permittivity ( $\epsilon''$ ) of the  $\text{Fe}_3\text{O}_4@ \text{CuSilicate}$  yolk-shell microspheres indicates the intense dielectric losses as compared with that of the pure  $\text{Fe}_3\text{O}_4$ , which may be ascribed to the well-defined hierarchical yolk-shell structure constructed by the nanoneedle shells. The maximum reflection loss value of the  $\text{Fe}_3\text{O}_4@ \text{CuSilicate}$  yolk-shell microspheres with 450-nm  $\text{Fe}_3\text{O}_4$  cores and 125-nm copper silicate shells is  $-23.5$  dB at 7 GHz with a thickness of 2 mm, and the absorption bandwidths with reflection loss lower than  $-10$  dB are up to 10.4 GHz.

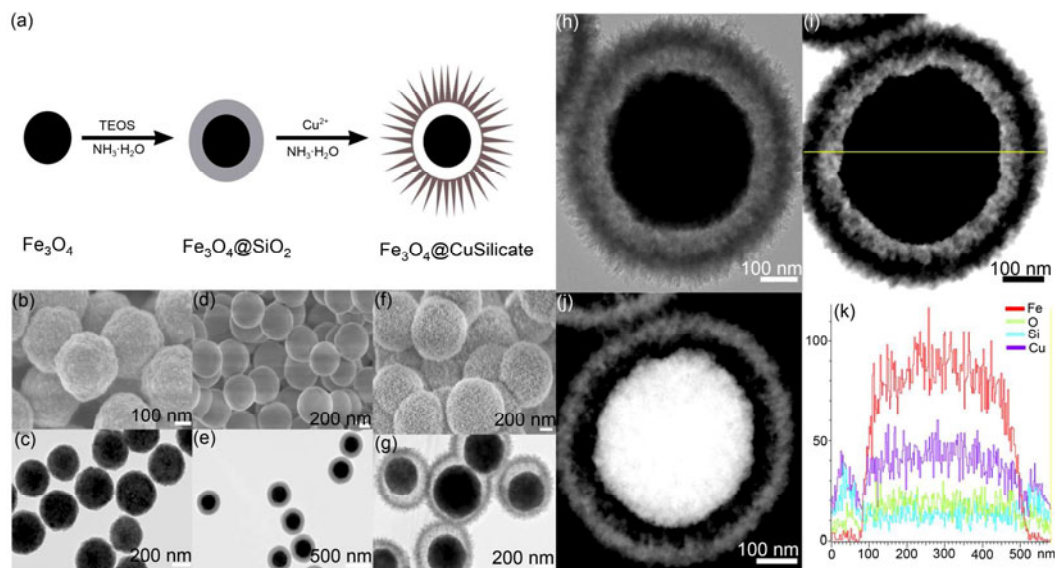


**Figure 4** (a) Schematic illustration of the synthesis procedure for the  $\text{Fe}_3\text{O}_4@CuSilicate$  yolk-shell microspheres. (b–g) TEM and FESEM images of the  $\text{Fe}_3\text{O}_4$  (b, c),  $\text{Fe}_3\text{O}_4@SiO_2$  core-shell microspheres (d, e) and  $\text{Fe}_3\text{O}_4@CuSilicate$  yolk-shell microspheres (f, g). TEM (h), BF-STEM (i), and HAADF-STEM (j) images of an individual yolk-shell microsphere. (k) Line scanning profiles of Fe, O, Si, and Cu recorded along the line shown in (i). (Copyright (2013) American Chemical Society)

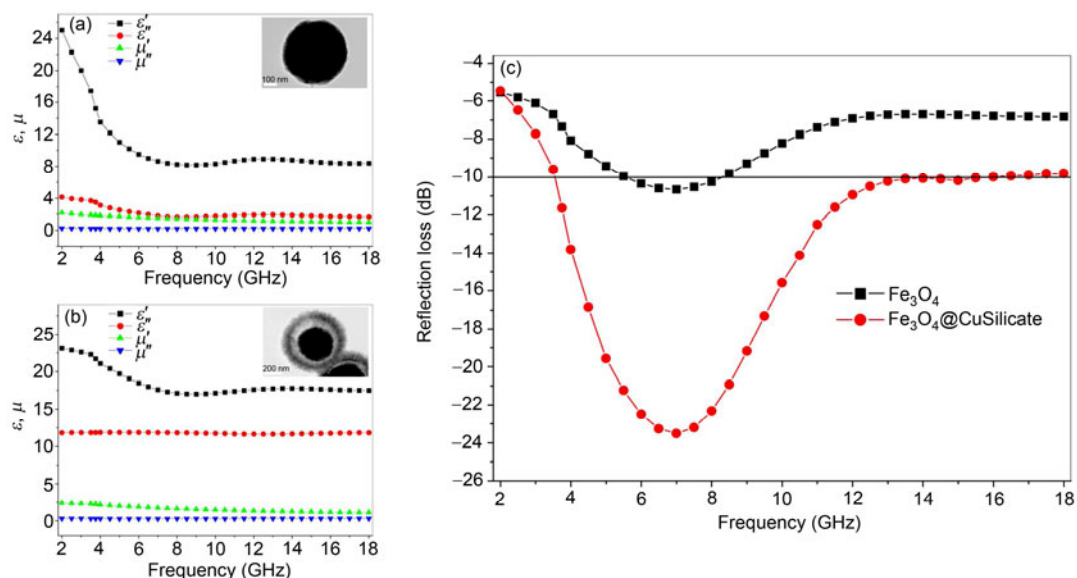


**Figure 5** (a) Frequency dependence of real ( $\epsilon'$ ) and imaginary ( $\epsilon''$ ) parts of complex permittivity and permeability of  $\text{Fe}_3\text{O}_4$  (a) and  $\text{Fe}_3\text{O}_4@CuSilicate$  yolk-shell microspheres (b). Microwave reflection loss curves of the  $\text{Fe}_3\text{O}_4$  and  $\text{Fe}_3\text{O}_4@CuSilicate$  yolk-shell microspheres (c). The insets in (a) and (b) show the TEM images of the corresponding  $\text{Fe}_3\text{O}_4$  (a) and  $\text{Fe}_3\text{O}_4@CuSilicate$  yolk-shell microspheres. (Copyright (2013) American Chemical Society)

## 5 Yolk-shell microspheres with $\text{Fe}_3\text{O}_4$ cores and $\text{SnO}_2$ double shells

To endow the yolk-shell structures with multi-functionalities and synergistic properties, considerable efforts have recently been devoted to rational design of the shells with desirable components, multi-layers, and well-defined structures [28]. For example, Zhao *et al.* [29] demonstrated a hydrothermal etching assisted crystallization route to synthesize

$\text{Fe}_3\text{O}_4@$  titanate yolk-shell microspheres with ultrathin nano sheet- assembled double-shell structure, which exhibited a remarkable catalytic performance. Wang and co-workers [30] developed a straightforward and general strategy to prepare metal oxide hollow microspheres with multiple shells for gas-sensing. Our previous work on the yolk-shell structures showed that it was possible to achieve significantly enhanced microwave absorption properties. This fact also intrigued us to design and synthesize the complex yolk-shell structures with optimized compositions and mul-

ti-shells via a facile approach.

More recently, we developed a facile and efficient strategy for the synthesis of double-shelled yolk-shell microspheres with  $\text{Fe}_3\text{O}_4$  cores and  $\text{SnO}_2$  double shells [31]. As shown in Figure 6(a), the double-shelled  $\text{Fe}_3\text{O}_4@/\text{SnO}_2$  yolk-shell microspheres were obtained by hydrothermal shell-by-shell deposition of  $\text{SnO}_2$  using  $\text{Fe}_3\text{O}_4@/\text{SiO}_2$  as templates and  $\text{K}_2\text{SnO}_3$  as a precursor. It can be seen in Figure 6(b) that the resulting microspheres were uniformly spherical and had a unique double-shelled yolk-shell structure with an average diameter of  $\sim 680$  nm. TEM image clearly indicated that the yolk-shell structure is composed of a dark core ( $\sim 330$  nm in diameter), an inner shell ( $\sim 66$  nm in thickness), an outer shell ( $\sim 51$  nm in thickness) and large interstitial void between the core and double shells (Figure 6(c)). EELS elemental mappings and corresponding RGB cropped imaging demonstrated the actual distribution of Fe, O, Sn elements in the microsphere, which further confirm the double-shelled yolk-shell structure with a  $\text{Fe}_3\text{O}_4$  core and  $\text{SnO}_2$  double shells (Figure 6(d–g)). The unique microstructure of these microspheres can be very useful for microwave absorption applications. First, the relatively large specific surface area ( $89 \text{ m}^2 \text{ g}^{-1}$ ) and high porosity ( $0.21 \text{ cm}^3 \text{ g}^{-1}$ ) as well as the void space existing in the double-shelled yolk-shell microspheres can provide more active sites for reflection and scattering of electromagnetic waves [32]. Second, the multiple core/shell/shell gradient interfac-

es are advantageous for electromagnetic attenuation due to the interfacial polarization [14, 33]. Third, the large void space between the  $\text{Fe}_3\text{O}_4$  core and  $\text{SnO}_2$  double shells can effectively interrupt the spread of electromagnetic waves and generate dissipation due to the existing impedance difference [34]. Fourth, the effective complementarities between the magnetic loss and dielectric loss, which originate from the synergistic effects of the  $\text{Fe}_3\text{O}_4$  core and  $\text{SnO}_2$  double shells, can be realized [13, 35, 36]. As expected, the maximum reflection loss value of the double-shelled  $\text{Fe}_3\text{O}_4@/\text{SnO}_2$  yolk-shell microspheres could reach  $-36.5$  dB at 7 GHz with a thickness of 2 mm, and the absorption bandwidths with reflection loss lower than  $-20$  dB are up to 8.5 GHz.

## 6 Yolk-shell microspheres with $\text{Fe}_3\text{O}_4$ cores and mixed barium silicate and barium titanium oxide shells

In order to further expand the application potential of the yolk-shell structures, it is very important to engineer the shells with unique morphologies, advanced chemical compositions and built-in functionalities [37]. However, most of the yolk-shell structures reported in previous studies were generally composed of single-component shells. Apparent-

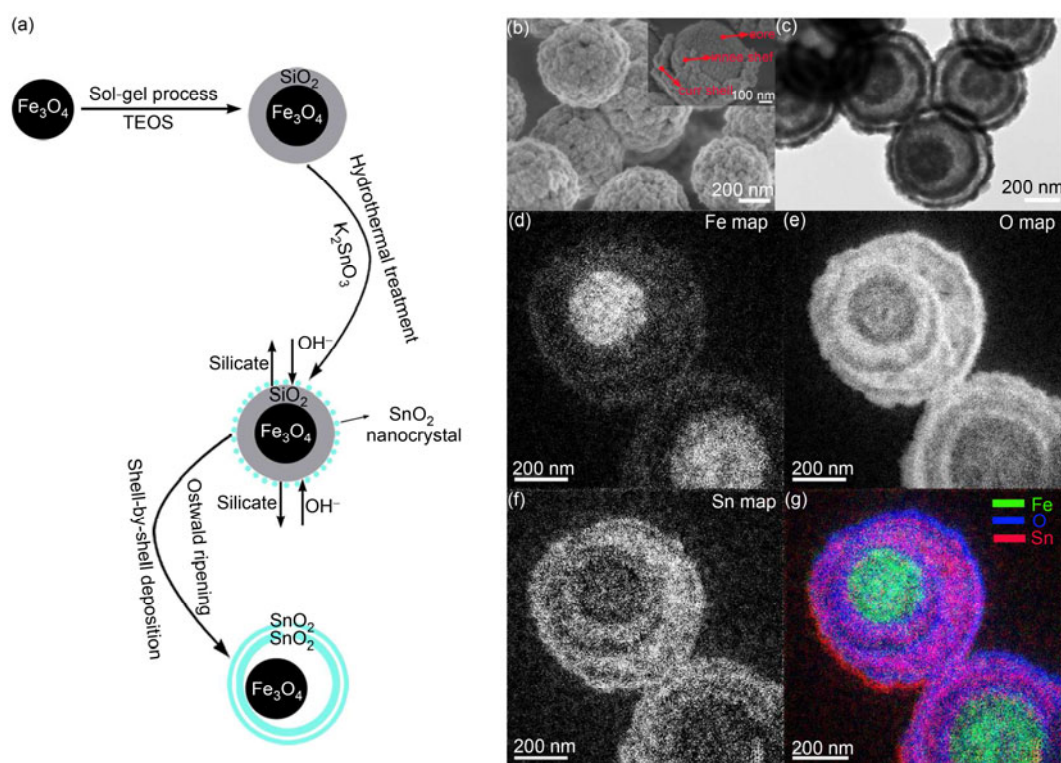


**Figure 6** (a) Schematic illustration of the formation process of the double-shelled  $\text{Fe}_3\text{O}_4@/\text{SnO}_2$  yolk-shell microspheres. (b) FESEM, (c) TEM, and (d–g) EELS elemental mappings and corresponding RGB cropped images of the double-shelled  $\text{Fe}_3\text{O}_4@/\text{SnO}_2$  yolk-shell microspheres. The inset in (b) shows a high-magnification FESEM image of a broken microsphere. (Copyright (2013) American Chemical Society)

ly, the complex yolk-shell structures with double- or multi-component shells may exhibit interesting chemistry as well as effective interfaces and material-dependent properties that are unique when compared to single-component shells, and therefore offer an avenue to obtain excellent absorption performance with these complex yolk-shell structures.

Inspired by this idea, we demonstrated a facile hydrothermal-assisted crystallization route to synthesize hierarchical yolk-shell microspheres with  $\text{Fe}_3\text{O}_4$  cores and mixed barium silicate and barium titanium oxide shells [38]. As illustrated in Figure 7(a), the synthesis procedure consists of three main steps: coating of  $\text{Fe}_3\text{O}_4$  particles with uniform shells of silica via the classical Stöber method, formation of  $\text{TiO}_2$  shells on  $\text{Fe}_3\text{O}_4@ \text{SiO}_2$  colloids through a sol-gel approach, and hydrothermal treatment in aqueous  $\text{Ba}(\text{OH})_2$  solution (Figure 7(b–g)). On the basis of time-dependent TEM observations of the hydrothermal process, we proposed a possible formation mechanism of these microspheres (Figure 7(h)). During hydrothermal reaction in the alkaline solution, a prior etching process preferentially occurs at the  $\text{SiO}_2/\text{TiO}_2$  interface of the  $\text{Fe}_3\text{O}_4@ \text{SiO}_2@ \text{TiO}_2$  microspheres due to different etching behavior of  $\text{SiO}_2$  and  $\text{TiO}_2$ , which could allow subsequent induced energy in the cavity. The etched silica parts would react with the  $\text{Ba}^{2+}$  cations to form the barium silicate nanograins and redeposit on the surface of the  $\text{SiO}_2$  layer because of Ostwald ripening. As the reaction progresses, the outer  $\text{TiO}_2$  layer may transform to the barium titanium oxide shell via the dissolution-precipitation and *in-situ* transformation processes. Consequently, the unique yolk-shell microspheres with a mixture shell of barium silicate and barium titanium oxide are formed. As shown in Figure 8, the maximum reflection loss

values for these microspheres increase by increasing the shell thickness, which could reach  $-37.6$  dB at 7 GHz at a thickness of 2 mm. The significantly enhanced microwave absorption properties may result from the complex yolk-shell structure with a large surface area and high porosity, as well as synergistic effects between the magnetic  $\text{Fe}_3\text{O}_4$  cores and mixed barium silicate and barium titanium oxide shells.

## 7 Non-spherical yolk-shell structures

It is well-known that the absorption properties of a material are closely related to its structure. The anisotropic particles may have a higher resonance frequency and exceed the Snoek's limit in the gigahertz frequency range owing to their large shape anisotropy, making these materials the ideal candidates for microwave absorption in relatively high frequency range [39].

To the best of our knowledge, most of the resulting yolk-shell structures are spherical in shape. Very little success has been achieved to construct non-spherical yolk-shell structures with well-defined shells, partly because of the paucity of non-spherical templates and difficulty in forming uniform coatings around high-curvature surfaces [40]. Morphology-controlled synthesis of non-spherical yolk-shell structures through a facile route is still a great challenge. Hence there exists a need for the development of nonspherical yolk-shell structures that could lead to significant improvements in microwave absorption performance. Figure 9 shows some experimental results for the design and synthesis of non-spherical yolk-shell structures. Utilizing

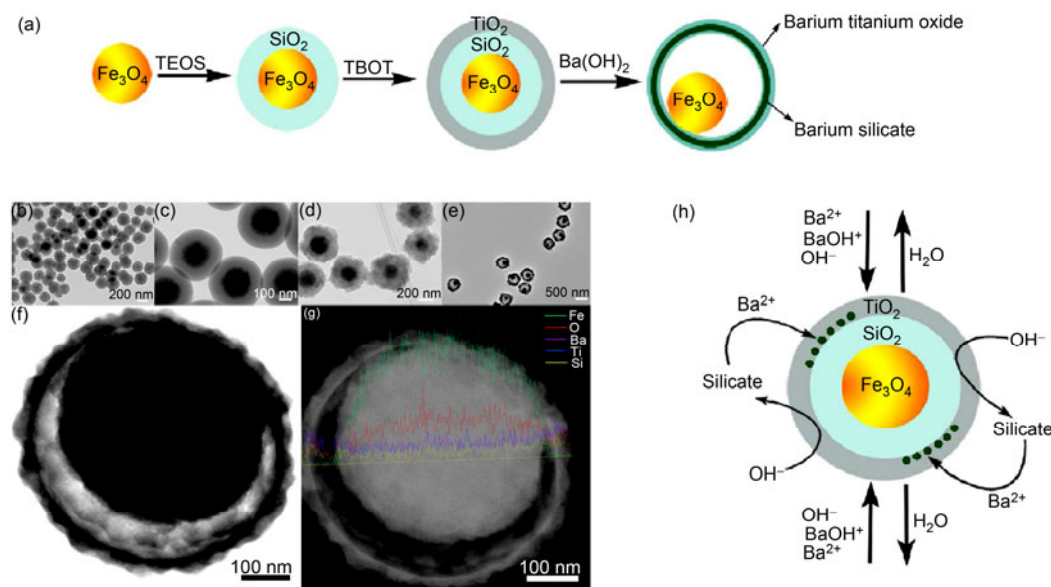


**Figure 7** (a) Schematic illustration of the synthesis procedure for the hierarchical yolk-shell microspheres with  $\text{Fe}_3\text{O}_4$  cores and mixed barium silicate and barium titanium oxide shells. (b–e) TEM images of the  $\text{Fe}_3\text{O}_4$  (b),  $\text{Fe}_3\text{O}_4@ \text{SiO}_2$  (c),  $\text{Fe}_3\text{O}_4@ \text{SiO}_2@ \text{TiO}_2$  (d), and yolk-shell microspheres (e). (f) BF-STEM and (g) HAADF-STEM images of an individual yolk-shell microsphere. (h) Schematic illustration of the “hydrothermal-assisted crystallization” strategy for the synthesis of the yolk-shell microspheres. (Reprinted by permission of The Royal Society of Chemistry (RSC))

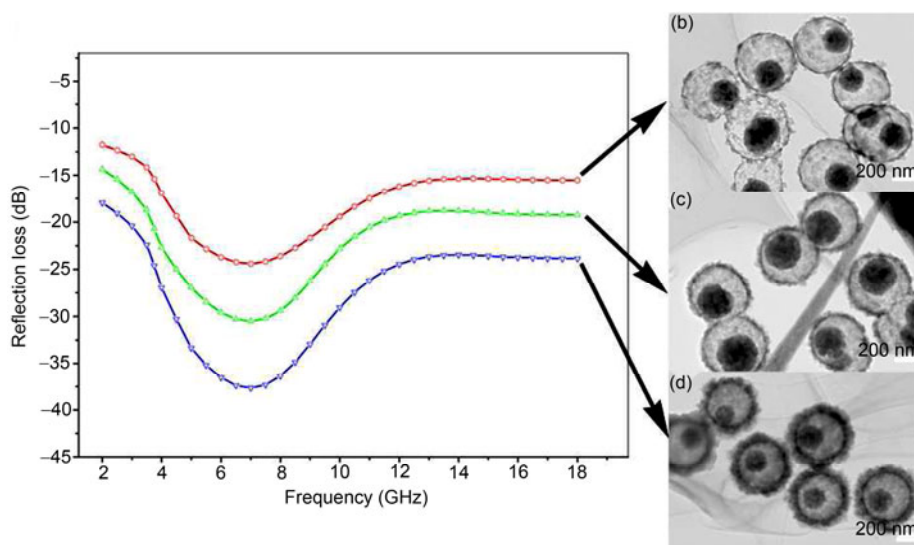


**Figure 8** (a) Microwave reflection loss curves of the hierarchical yolk-shell microspheres with  $\text{Fe}_3\text{O}_4$  cores and mixed barium silicate and barium titanium oxide shells and (b–d) TEM images of the corresponding yolk-shell microspheres with different shell thicknesses. (Reprinted by permission of The Royal Society of Chemistry (RSC))

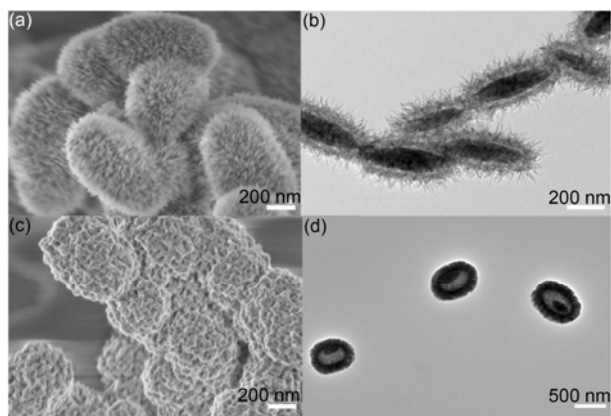


**Figure 9** FESEM (a, c) and TEM (b, d) images of the non-spherical yolk-shell structures.

the same template-assisted method but employing  $\alpha\text{-Fe}_2\text{O}_3$  as the starting template, ellipsoidal yolk-shell structures with  $\alpha\text{-Fe}_2\text{O}_3$  cores and hierarchical shells were prepared first, followed by the transformation from the  $\alpha\text{-Fe}_2\text{O}_3$  to  $\text{Fe}_3\text{O}_4$  in  $\text{H}_2$  atmosphere. Based on these preliminary results we expect that more complex and promising yolk-shell structures could be synthesized by using the sol-gel template-assisted methods.

## 8 Mechanism discussion

The excellent microwave absorption performance may be attributed to the unique nanostructure of the magnetic  $\text{Fe}_3\text{O}_4$ @oxide nano-structures. Firstly, as calculated by the BET method, such a core@shell structure gives rise to a higher BET surface area and a relatively high pore volume,

respectively. Thus, the relatively large specific surface area and high porosity, as well as the large internal void of these nano-composites can provide more active sites for reflection and scattering of electromagnetic wave. Secondly, the well-defined shells constructed by hierarchical nano-structures may generate a high dielectric constant and loss, while the dominant dipolar polarization and the associated relaxation phenomena contribute to the loss mechanisms. Thirdly, the effective complementarities between the magnetic loss and the dielectric loss, which originate from the synergistic effect of the  $\text{Fe}_3\text{O}_4$ -based cores and different types of oxide shells, can be realized. The EM impedance matching is more satisfied, which are responsible for the significantly enhanced microwave absorption properties.

## 9 Conclusions and outlook

In conclusion, we have summarized the recent advances in design and synthesis of hierarchical  $\text{Fe}_3\text{O}_4$ -based core-shell or yolk-shell nanostructures as microwave absorbers for microwave absorption applications. It can be concluded that the microwave absorption properties of  $\text{Fe}_3\text{O}_4$ -based absorbers can be effectively enhanced by making proper nanostructures with optimized chemical compositions. Using  $\text{Fe}_3\text{O}_4$  as an example, we highlight the importance of the unique core-shell or yolk-shell nanostructures on the microwave absorption properties of the material. Such concepts and strategies can be extended to other potential materials, thus shedding some light on the future development of high-efficient absorbers. In addition, several future trends in this field are discussed herein. Nowadays, a large part of efforts still focus on the combination of different absorption agents in order to achieve a novel absorber with strong ab-



sorption intensity and wide absorption frequency range. While, more and more research interest is paid to the design of new nanostructure to obtain satisfactory microwave absorption performance. Some new structure designed as microwave absorption agent by other group is inspiring. For example, Zhuo *et al.* [41] developed a ZnO dendritic nanostructures and their result showed that the dendritic structure played an important role for the absorption performance. Even though great research efforts have been made, the prepared microwave absorber with strong absorption in a broad frequency range still remains challenging. Besides the synthesis of advanced absorption materials, it is also highly necessary to study the related fundamental scientific issues. For instance, it is important to understand the absorption mechanisms of the nanostructures and to investigate the physical/chemical properties of interfaces as well as their effects on the absorption performance. Finally, large-scale preparation methods should be developed for practical utilization of the nanostructures. Despite those challenges, we believe that there will be significant improvement for the microwave absorption properties of multifunctional nanostructures along with the advances in the related fabrication and characterization techniques.

This work was supported by the National Natural Foundation of China (11274066, 51172047, 50872145 and 51102050), the National Basic Research Program of China (973 Program, 2013CB932901 and 2009CB930803), and the project sponsored by Shanghai Pujiang Program and "Shu Guang" project of Shanghai Municipal Education Commission and Shanghai Education Development Foundation (09SG01).

- Kim J, Piao Y, Hyeon T. Multifunctional nanostructured materials for multimodal imaging, and simultaneous imaging and therapy. *Chem Soc Rev*, 2009, 38: 372–390
- Hammond PT. Form and function in multilayer assembly: New applications at the nanoscale. *Adv Mater*, 2004, 16(15): 1271–1293
- Wu S, Dzubiella J, Kaiser J, Drechsler M, Guo X, Ballauff M, Lu Y. Thermosensitive Au-PNIPAA yolk-shell nanoparticles with tunable selectivity for catalysis. *Angew Chem Int Ed*, 2012, 51(9): 2229–2233
- Zhai X, Yu M, Cheng Z, Hou Z, Yang D, Kang X, Dai Y, Wang D, Lin J. Rattle-type hollow  $\text{CaWO}_4$ :  $\text{Tb}^{3+}$ @ $\text{SiO}_2$  nanocapsules as carriers for drug delivery. *Dalton Trans*, 2011, 40(48): 12818–12825
- Liu J, Qiao SZ, Chen JS, Lou XW, Xing X, Lu GQ. Yolk/shell nanoparticles: New platforms for nanoreactors, drug delivery and lithium-ion batteries. *Chem Commun*, 2011, 47(47): 12578–12591
- Lee I, Joo JB, Yin Y, Zaera F. A yolk@shell nanoarchitecture for Au/TiO<sub>2</sub> catalysts. *Angew Chem Int Ed*, 2011, 50(43): 10208–10211
- Yan LA, Zhao F, Li SJ, Hu ZB, Zhao YL. Low-toxic and safe nanomaterials by surface-chemical design, carbon nanotubes, fullerenes, metallofullerenes, and graphenes. *Nanoscale*, 2011, 3(2): 362–382
- Lou XW, Li CM, Archer LA. Designed synthesis of coaxial  $\text{SnO}_2$ @carbon hollow nanospheres for highly reversible lithium storage. *Adv Mater*, 2009, 21(24): 2536–2539
- Huo J, Wang L, Yu H. Polymeric nanocomposites for electromagnetic wave absorption. *J Mater Sci*, 2009, 44(15): 3917–3927
- Wang L, Wu H, Shen Z, Guo S, Wang Y. Enhanced microwave absorption properties of Ni-doped ordered mesoporous carbon/polyaniline nanocomposites. *Mater Sci Eng B*, 2012, 177(18): 1649–1654
- Li N, Cao MH, Hu CW. A simple approach to spherical nickel-carbon monoliths as light-weight microwave absorbers. *J Mater Chem*, 2012, 22(35): 18426–18432
- Xu MH, Zhong W, Qi XS, Au CT, Deng Y, Du YW. Highly stable Fe-Ni alloy nanoparticles encapsulated in carbon nanotubes: Synthesis, structure and magnetic properties. *J Alloys Compd*, 2010, 495(1): 200–204
- Zhou M, Zhang X, Wei J, Zhao S, Wang L, Feng B. Morphology-controlled synthesis and novel microwave absorption properties of hollow urchinlike  $\alpha$ - $\text{MnO}_2$  nanostructures. *J Phys Chem C*, 2010, 115(5): 1398–1402
- Zhu CL, Zhang ML, Qiao YJ, Xiao G, Zhang F, Chen YJ.  $\text{Fe}_3\text{O}_4$ /TiO<sub>2</sub> core/shell nanotubes: Synthesis and magnetic and electromagnetic wave absorption characteristics. *J Phys Chem C*, 2010, 114(39): 16229–16235
- Chen YJ, Gao P, Wang RX, Zhu CL, Wang LJ, Cao MS, Jin HB. Porous  $\text{Fe}_3\text{O}_4$ /SnO<sub>2</sub> core/shell nanorods: Synthesis and electromagnetic properties. *J Phys Chem C*, 2009, 113(23): 10061–10064
- Chen YJ, Zhang F, Zhao GG, Fang XY, Jin HB, Gao P, Zhu CL, Cao MS, Xiao G. Synthesis, Multi-nonlinear dielectric resonance, and excellent electromagnetic absorption characteristics of  $\text{Fe}_3\text{O}_4$ /ZnO core/shell nanorods. *J Phys Chem C*, 2010, 114(20): 9239–9244
- Wang FL, Liu JR, Kong J, Zhang ZJ, Wang XZ, Itoh M, Machida K. Template free synthesis and electromagnetic wave absorption properties of monodispersed hollow magnetite nano-spheres. *J Mater Chem*, 2011, 21(12): 4314–4320
- Liu J, Qiao SZ, Hu QH, Lu GQ. Magnetic nanocomposites with mesoporous structures: synthesis and applications. *Small*, 2011, 7: 425–443
- Yan SJ, Zhen L, Xu CY, Jiang JT, Shao WZ, Tang JK. Synthesis, characterization and electromagnetic properties of  $\text{Fe}_{1-x}\text{Co}_x$  alloy flower-like microparticles. *J Magn Magn Mater*, 2011, 323(5): 515–520
- Liu J, Che R, Chen H, Zhang F, Xia F, Wu Q, Wang M. Microwave absorption enhancement of multifunctional composite microspheres with spinel  $\text{Fe}_3\text{O}_4$  cores and anatase TiO<sub>2</sub> shells. *Small*, 2012, 8(8): 1214–1221
- Liu JW, Xu JJ, Che RC, Chen HJ, Liu MM, Liu ZW. Hierarchical  $\text{Fe}_3\text{O}_4$ @TiO<sub>2</sub> yolk-shell microspheres with enhanced microwave-absorption properties. *Chem Eur J*, 2013, 19(21): 6746–6752
- Wu XJ, Xu D. Formation of yolk/SiO<sub>2</sub> shell structures using surfactant mixtures as template. *J Am Chem Soc*, 2009, 131(8): 2774–2775
- Suzuki T, Okazaki KI, Suzuki S, Shibayama T, Kuwabata S, Torimoto T. Nanosize-controlled syntheses of indium metal particles and hollow indium oxide particles via the sputter deposition technique in ionic liquids. *Chem Mater*, 2010, 22(18): 5209–5215
- Yin Y, Rioux RM, Erdonmez CK, Hughes S, Somorjai GA, Alivisatos AP. Formation of hollow nanocrystals through the nanoscale kirckendall effect. *Science*, 2004, 304(5671): 711–714
- Fang Q, Xuan S, Jiang W, Gong X. Yolk-like micro/nanoparticles with superparamagnetic iron oxide cores and hierarchical nickel silicate shells. *Adv Funct Mater*, 2011, 21(10): 1902–1909
- Zhao W, Chen H, Li Y, Li L, Lang M, Shi J. Uniform Rattle-type hollow magnetic mesoporous spheres as drug delivery carriers and their sustained-release property. *Adv Funct Mater*, 2008, 18(18): 2780–2788
- Liu JW, Cheng J, Che RC, Xu JJ, Liu MM, Liu ZW. Synthesis and microwave absorption properties of yolk-shell microspheres with magnetic iron oxide cores and hierarchical copper silicate shells. *ACS Appl Mater Interfaces*, 2013, 5: 2503–2509
- Kim M, Sohn K, Na BH, Hyeon T. Synthesis of nanorattles composed of gold nanoparticles encapsulated in mesoporous carbon and polymer shells. *Nano Lett*, 2002, 2(12): 1383–1387
- Li W, Deng YH, Wu ZX, Qian XF, Yang JP, Wang Y, Gu D, Zhang F, Tu B, Zhao DY. Hydrothermal etching assisted crystallization: A facile route to functional yolk-shell titanate microspheres with ultrathin nanosheets-assembled double shells. *J Am Chem Soc*, 2011, 133: 15830–15833
- Lai X, Li J, Korgel BA, Dong Z, Li Z, Su F, Du J, Wang D. General

- Synthesis and gas-sensing properties of multiple-shell metal oxide hollow microspheres. *Angew Chem Int Ed*, 2011, 123(12): 2790–2793
- 31 Liu JW, Cheng J, Che RC, Xu JJ, Liu MM, Liu ZW. Double-shelled yolk-shell microspheres with  $\text{Fe}_3\text{O}_4$  cores and  $\text{SnO}_2$  double shells as high-performance microwave absorbers. *J Phys Chem C*, 2013, 117(1): 489–495
- 32 Qin Y, Che RC, Liang CY, Zhang J, Wen ZW. Synthesis of Au and Au-CuO cubic microcages via an in situ sacrificial template approach. *J Mater Chem*, 2011, 21(11): 3960–3965
- 33 Sun G, Dong B, Cao M, Wei B, Hu C. Hierarchical dendrite-like magnetic materials of  $\text{Fe}_3\text{O}_4$ ,  $\gamma\text{-Fe}_2\text{O}_3$ , and Fe with high performance of microwave absorption. *Chem Mater*, 2011, 23(6): 1587–1593
- 34 Guo XH, Deng YH, Gu D, Che RC, Zhao DY. Synthesis and microwave absorption of uniform hematite nanoparticles and their core-shell mesoporous silica nanocomposites. *J Mater Chem*, 2009, 19(37): 6706–6712
- 35 Zhou J, He J, Li G, Wang T, Sun D, Ding X, Zhao J, Wu S. Direct incorporation of magnetic constituents within ordered mesoporous carbon-silica nanocomposites for highly efficient electromagnetic wave absorbers. *J Phys Chem C*, 2010, 114(17): 7611–7617
- 36 Chen YJ, Gao P, Zhu CL, Wang RX, Wang LJ, Cao MS, Fang XY. Synthesis, magnetic and electromagnetic wave absorption properties of porous  $\text{Fe}_3\text{O}_4/\text{Fe}/\text{SiO}_2$  core/shell nanorods. *J Appl Phys*, 2009, 106(5): 054303–054304
- 37 Wu XJ, Xu D. Soft template synthesis of yolk/silica shell particles. *Adv Mater*, 2010, 22(13): 1516–1520
- 38 Liu JW, Xu JJ, Che RC, Chen HJ, Liu ZW, Xia F. Hierarchical magnetic yolk-shell microspheres with mixed barium silicate and barium titanium oxide shells for microwave absorption enhancement. *J Mater Chem*, 2012, 22(18): 9277–9284
- 39 Yang RB, Liang WF. Microwave properties of high-aspect-ratio carbonyl iron/epoxy absorbers. *J Appl Phys*, 2011, 109(7): 07A311–313
- 40 Wang Z, Zhou L, Lou XW. Metal oxide hollow nanostructures for lithium-ion batteries. *Adv Mater*, 2012, 24(14): 1903–1911
- 41 Zhuo RF, Feng HT, Chen JT, Yan D, Feng JJ, Li HJ, Geng BS, Cheng S, Xu XY, Yan PX. Multistep synthesis, growth mechanism, optical, and microwave absorption properties of ZnO dendritic nanostructures. *J Phys Chem C*, 2008, 112(31): 11767–11775